JOURNAL OF MATERIALS SCIENCE 32 (1997) 4077–4084

Tensile test for estimation of thermal fatigue properties of solder alloys

T. TAKEMOTO, A. MATSUNAWA
Joining and Welding Research Institute, Osaka University, Ibaraki, Osaka 567, Japan
M. TAKAHASHI
Graduate School, Osaka University, Suita, Osaka 565, Japan

A tensile test is proposed to evaluate the thermal fatigue resistance of solder alloys. The test is based on the strain rate change method to obtain the strain rate sensitivity index, m. The m value is obtained at various strains during the tensile test. The plots of m and strain where m is measured showed a linear relation; therefore, the m value at zero strain, m_0, and the gradient, k, are obtained by extrapolation. The m value at zero strain related to the coarseness or fineness of solder alloy microstructure; m_0 becomes lower with coarsening of the microstructure. The solder alloys with low m_0 and low k have excellent thermal fatigue resistance when compared with alloys with high m_0 and high k. m_0 and k would be good measures to estimate the thermal fatigue properties of solder alloys; highly resistant alloys have low m_0 and low k.

1. Introduction

Tin–lead eutectic solder alloys with 37–40 mass% Pb are essential materials for microsoldering in electronics assembly because of their excellent wettability and other necessary properties such as melting temperature and surface tension. In the recent high-density surface mount technology [1–4], the density of components assembled on board per unit area is increasing continuously, which causes severe conditions for solders. The surface mounting forced the solders as construction materials to sustain components; the high-density mounting and the use of high functional components produce high heat generation from components [2] which increases the ambient temperature during the use of electronics. These conditions cause higher risk of thermal fatigue damage in solder alloys. To improve the thermal fatigue properties (TFPs), it is important to change the design of board and solder land, and to adjust the thermal expansion coefficient of the materials. Conventional Sn–Pb eutectic solder has been believed to have the worst resistance to thermal fatigue [5]; therefore, the substitution of solder and the modification of solder alloys by the addition of some elements are also effective in improving the TFPs of solder joints. Alloys with single-phase structure and dispersion-hardened alloys are thought to possess higher resistance [5]. In practice, the use of Sn–Ag and Sn–Sb alloys is effective in securing a longer thermal fatigue life [6].

The microstructure of Sn–Pb eutectic alloy coarsened after thermal fatigue; large tin and lead solid solution phases were observed, especially near the propagating cracks [6, 7]. During holding even at room temperature, the microstructures of solder alloys coarsen [8] because room temperature is much higher than 60% of the absolute melting temperature, T_m; the rise in holding temperature enhances the coarsening rate. In general, many alloys with a fine microstructure have excellent mechanical properties; therefore, suppression of the coarsening is believed to enhance the thermal fatigue resistance of solder alloys. The addition of several elements to Sn–Pb solder alloy was found to be effective [9, 10].

On the other hand, the use of lead in electronic assemblies is expected to be prohibited because of its toxic effect [11, 12]. Investigations of new lead-free solders are proceeding to give the solders excellent solderability and the same melting temperature range of around 460 K [13, 14]. To establish the appropriate substitutional lead-free solder, it is important that the new solder developed should have excellent TFPs. Thermal fatigue testing requires a long time and the manufacturing of test boards; therefore, it is very useful if the TFPs of solder alloys could be estimated by a simple mechanical test.

Sn–Pb alloy has been known to exhibit superplasticity; the strain rate sensitivity index (SRSI) is a measure of superplasticity [15–18] which is closely related to the microstructure including the grain size. As mentioned earlier, the fine microstructure is believed to possess high TFPs, and creep behaviour [19–24] also relates to the thermal fatigue life; therefore, the SRSI would be effective for comparing the relation between the microstructure and TFPs. In this work, a tensile test to obtain the SRSI is proposed to estimate the TFPs of solder alloys.

2. Experimental procedures

The solders used are several Sn–Pb alloys, Pb–In and Sn–3.5Ag as listed in Table I. The ranking of the

0022–2461

TABLE I Nominal chemical compositions of solder alloys for tensile tests

Solder alloy	Amount of element (mass%)					Ranking of TFP, [5]
	Sn	Ag	Sb	In	Pb	
Sn–37Pb	63	—	—	—	Balance	Worst
SnPb–Ag–Sn	62	0.7	0.6	—	Balance	Poor
Sn–36Pb–2Ag	62	2	—	—	Balance	Poor
Sn–10Pb	90	—	—	—	Balance	Fair
Pb–50ln	—	—	—	50	Balance	Good
Sn–3.5Ag	96.5	3.5	—	—	—	Excellent

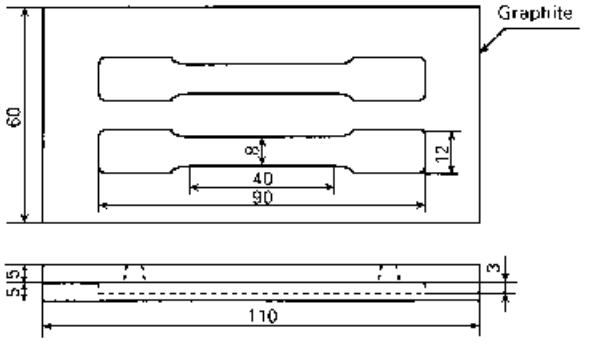

Figure 1 Shape and size of graphite crucible for making cast tensile test specimens. The dimensions are in millimetres.

thermal fatigue resistance of the alloys according to [5] is also indicated in the table. In the first stage of the study, two Sn–37Pb alloys, one plane eutectic without additional elements and the other containing small amounts of silver and antimony, are used to establish the basic procedure for the test and the meaning of parameters such as the SRSI. The former alloy is called eutectic solder (Sn–Pb), and the latter alloyed solder (SnPb–Ag–Sb). The TFPs of these two solder alloys have been separately investigated by us previously [9]; the study revealed that the alloyed solder had superior TFPs to the eutectic solder. After 400 cycles of testing between 233 and 353 K on through-hole lands of a connector with eight pins, the number of cracked solder lands in alloyed solder was about one tenth when compared with eutectic solder. The ranking of the alloyed solder is not listed in [5]; however, the alloy is ranked as "poor" judging from the composition.

Fig. 1 shows the shape and size of the tensile test specimens. Specimens were made from high-purity metals and cast in a graphite crucible with extra heads at both ends. The cooling rate during solidification was about 1 K s^{-1}. After removal of extra heads, specimens were tested at room temperature using an Instron-type tensile-testing machine under a cross-head speed of 2 mm s^{-1} and a strain rate of 8.67×10^{-4} s^{-1}. To obtain the SRSI, m, the cross-head speed was changed to 0.2 mm s^{-1}, with a strain rate of 8.67×10^{-5} s^{-1}, repeatedly until fracture.

Fig. 2a explains the procedure for calculating m using a typical stress–strain curve of a solder. At certain strain, the cross-head speed is lowered; then the speed is reversed to the former rate after the flow stress

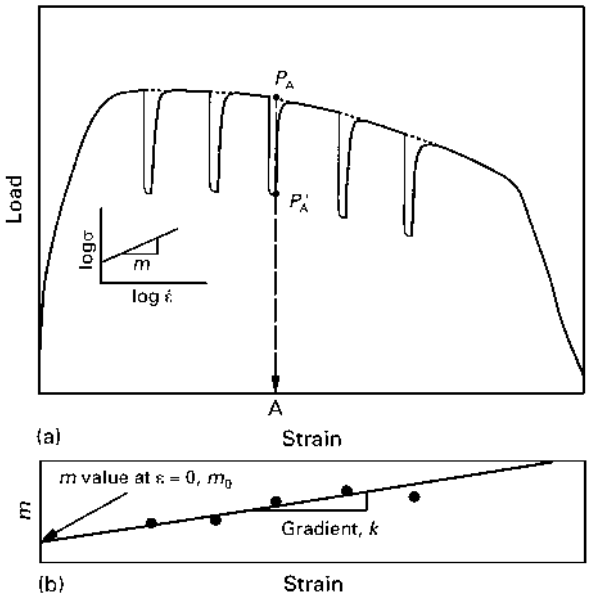

Figure 2 (a) Schematic diagram for obtaining the m value during variable-strain-rate tensile test ((—), $\dot{\varepsilon} = 8.3 \times 10^{-4}$ s^{-1}; (—), $\dot{\varepsilon}' = 8.3 \times 10^{-5}$ s^{-1}) and (b) the plot of m against strain where m is calculated to obtain m_0 and the gradient, k. $\sigma = a\dot{\varepsilon}^m$; $m = \log(P_A/P'_A)/\log(\dot{\varepsilon}/\dot{\varepsilon}')$.

reached almost steady state. The flow stresses P_A and P'_A, at the same strain, are measured for the calculation of m. The obtained m is plotted against the strain where the m is measured. The m was calculated from the following equation:

$$m = \frac{\log(P_1/P_2)}{\log(v_1/v_2)}$$

where P_1 is the stress under a cross-head speed, $v_1 = 2$ mm s^{-1} (strain rate of 8.67×10^{-4} s^{-1}) and P_2 is the stress under a cross-head speed, $v_2 = 0.2$ mm s^{-1} (strain rate of 8.67×10^{-5} s^{-1}).

The plots between m and strain showed an almost linear relationship within the range of the present work (Fig. 2b); the m at strain zero, m_0, is obtained by extrapolating the relation between m and the strain where m is measured. Tensile strength and elongation were also measured.

To investigate the stability of microstructure, the alloys were aged in oil baths at 353 and 393 K for up to 1800 ks. In the present paper, the as-cast condition means that the alloys were aged at room temperature for 10 days after casting into the shape shown in Fig. 1. The fineness of the microstructure is evaluated from the phase-to-phase distance (PPD). The PPD is obtained by measuring the number of cross-points between lead and tin phases in a straight line drawn on a scanning electron micrograph. The phases existing in alloyed solder were identified by X-ray diffractometry. The distribution of alloying elements was investigated by electron probe microanalysis.

3. Experimental results and discussion

Fig. 3 indicates the mechanical properties of solder alloys obtained by tensile testing. The alloyed solder

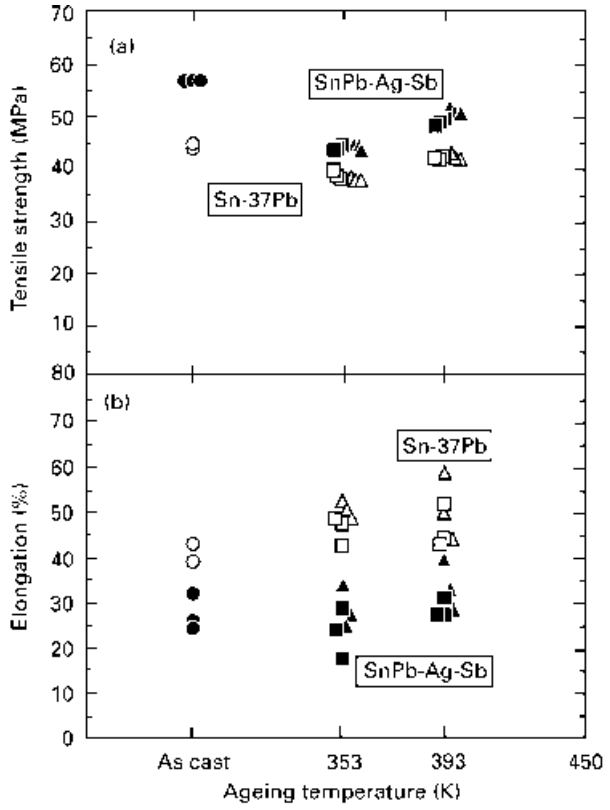

Figure 3 Mechanical properties of Sn–37Pb and SnPb–Ag–Sb solder alloys, showing (a) tensile strength and (b) elongation for various ageing times. Sn–37Pb, as cast; (□), Sn–37Pb, 605 ks; (△), Sn–37Pb, 1800 ks; SnPb–Ag–Sb, as cast; (■), SnPb–Ag–Sb, 605 ks (▲), SnPb–Ag–Sb, 1800 ks.

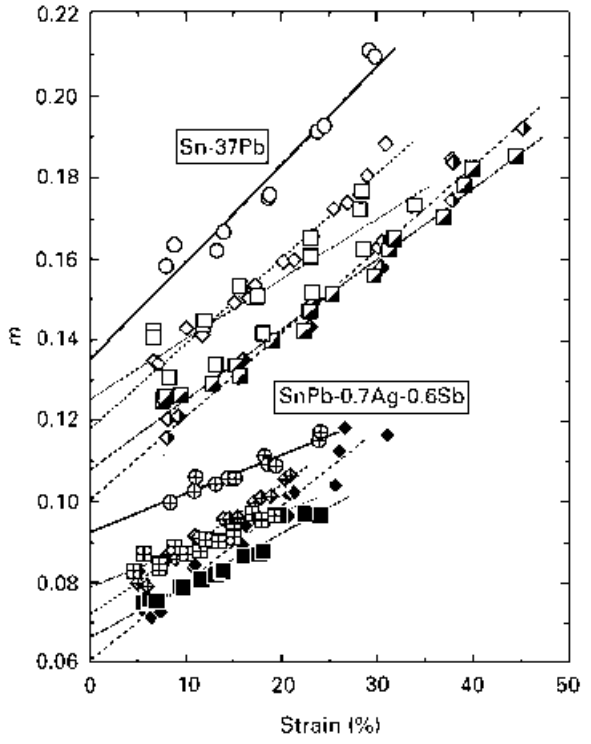

Figure 4 Plots of m versus strain (where m is measured) for various ageing conditions. (○), (⊕), as cast; (□), (■), 353 K, 605 ks; (◇), (◆), 393 K, 605 ks; (◪), (■), 353 K, 1800 ks; (◑), (◆), 393 K, 1800 ks.

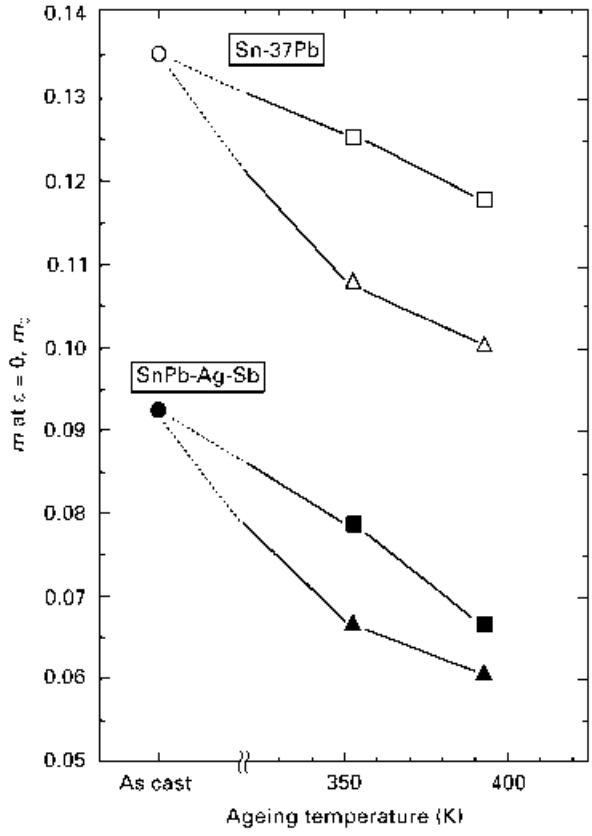

Figure 5 Changes in m_0 during ageing at 353 and 393 K. Sn–37Pb, as cast; (□), Sn–37Pb, 605 ks; (△), Sn–37Pb 1800 ks; SnPb–Ag–Sb, as cast; (■), SnPb–Ag–Sb, 605 ks (▲), SnPb–Ag–Sb, 1800 ks.

has an almost 25% higher tensile strength than the eutectic solder in the as-cast condition. Ageing at an elevated temperature lowered the strength but the holding time had no significant effect on the tensile strength. The decrease in strength is larger for low-temperature ageing, but the reason is not clear. In all ageing conditions, the alloyed solder maintained a higher strength. The alloyed solder had less elongation than the eutectic solder, and the elongation is almost constant irrespective of ageing conditions. The elongation of the eutectic solder increased with increase in the ageing temperature. In both alloys, elongation is almost independent of the holding time.

It is known that the addition of antimony raised both the hardness of various Sn–Pb solders [24] and the tensile strength of joints [25]. Our earlier work [9] revealed that the added antimony dissolved in tin gave a solid solution, resulting in solution hardening of alloyed solder. Silver formed finely dispersed Ag_3Sn intermetallic compounds; it is also responsible for the higher strength obtained by dispersion of hard intermetallic Ag_3Sn phase. The high tensile strength would be effective in improving the TFPs, because the thermal fatigue test is of the strain-controlled type, which forces solders to deform during thermal cycling through stress-relaxation-type creep. Accordingly, solders with a higher strength and large elongation are preferable in accordance with general materials. The alloyed solder had a higher strength but a smaller elongation; therefore, it is rather difficult to explain the excellent TFPs of alloyed solder from the mechanical properties.

Fig. 4 shows plots of m against the strain where the m value was measured. In all ageing conditions, the

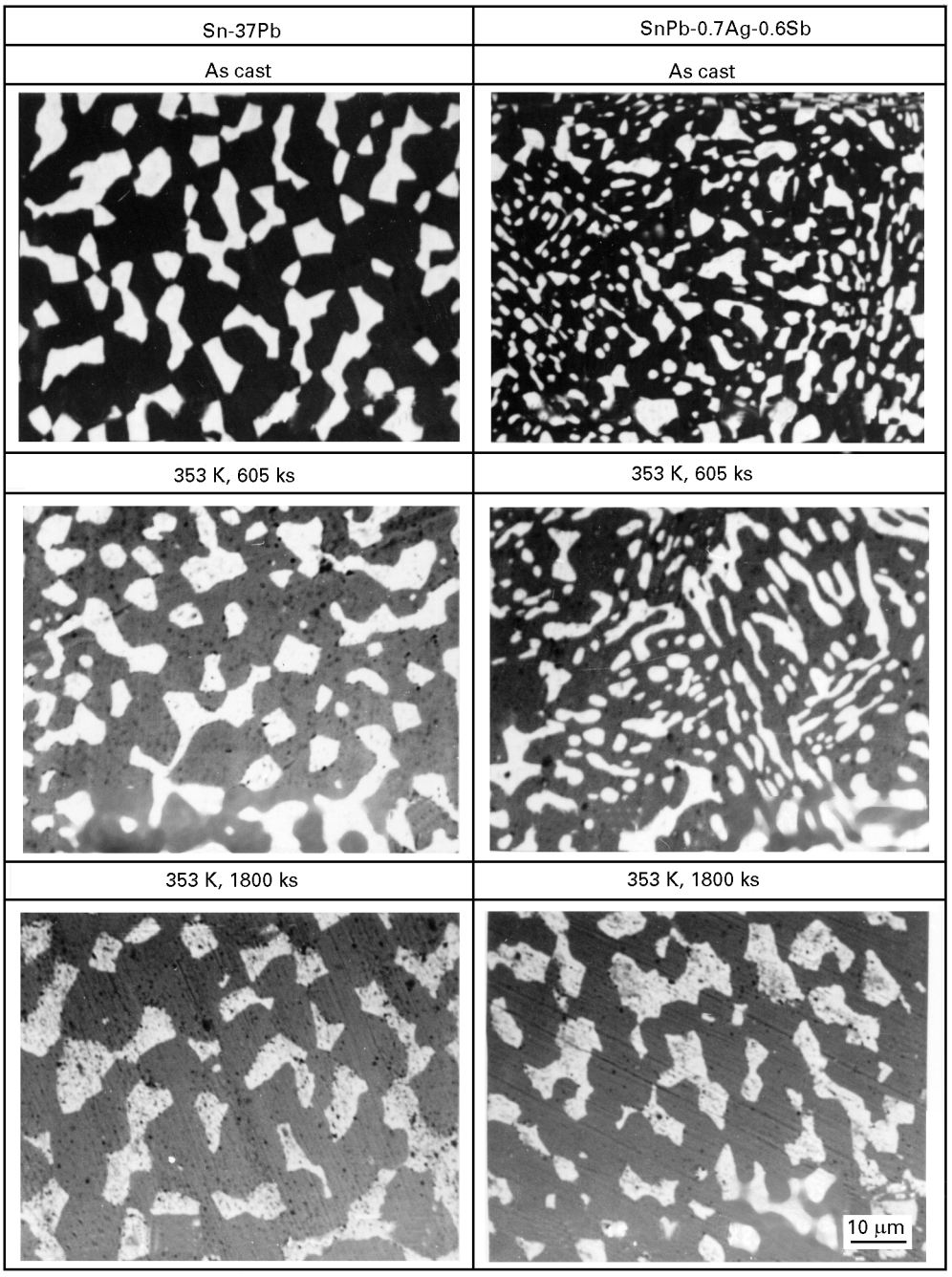

Figure 6 Coarsening of microstructure during heating at 353 K, as shown by the back-scattered electron image (composition).

plots show almost linear relations; then the m value at zero strain, m_0, and the gradient of the straight line, k, were obtained by extrapolating the straight line towards zero strain using the least-squares method. The m values for eutectic solder are always larger than those for alloyed solder. The gradient is also larger for eutectic solder. Ageing at an elevated temperature changed both the m value and the gradient in each solder.

Fig. 5 shows plots of the m value at zero strain, m_0, versus ageing temperature. In both alloys, m_0 became lower with increasing ageing temperature; also it decreased for longer holding times. The m_0 for eutectic solder is always larger than that for the alloyed solder in all ageing conditions. The gradient of the straight line also larger for eutectic solder in all ageing conditions (Fig. 4); therefore, these values would be a good measure for evaluating the TFPs of solder alloys; the alloys with lower m_0 and k might have a superior resistance to thermal fatigue than do the alloys with higher m_0 and k.

Ageing at an elevated temperature coarsened the microstructure. Fig. 6 shows the back-scattered electron image (composition) at different ageing conditions. In both alloys, the microstructure evolved with ageing time. The alloyed solder always maintained a finer structure than did the eutectic solder. The decrease in m_0 with ageing corresponds to the coarsening of microstructure. The plots of m_0 against average PPD is shown in Fig. 7. In both solders, m_0 decreased with increasing PPD, which means coarsening of the microstructure. The decreasing rate of m_0 with increase in PPD is larger in the eutectic solder. The m_0 values for the alloyed solder are always smaller

than those of the eutectic solders, i.e., m_0 is a characteristic value for each solder; it is different depending on the solder composition even at the same PPD.

The m value has been used to evaluate the superplasticity, the alloys with more than 0.3 often behave as superplastic materials [17]. In fact, Sn–Pb solder alloys in the as-cast condition usually do not have superplasticity. The solders used in this test had $m_0 < 0.14$, indicating that the deformation is not superplastic in the present test conditions. In this work, the strain rate was lowered during the tensile test; then a high m_0 means a large drop in stress when held at a lower strain rate, which means that the alloy with high m_0 has a high creep rate, because at a lower strain rate a longer time is required to give the same strain, resulting in a higher stress relaxation than at a higher strain rate.

The meaning of the gradient k can be considered as follows. The alloys with high k will behave as high-creep-rate materials after deformation proceeded, because the m_0 for the alloy rapidly increases with increasing strain. On the contrary, the alloys with low k maintain almost the same m value after deformation, which indicates a constant low creep rate irrespective of strain. Accordingly, low m_0 and low k mean a low creep rate. Thus, the alloys with low m_0 and k might have better resistance to thermal fatigue than do the alloys with high m_0 and k. To confirm this relation, several solder alloys with ranked TFPs were tested.

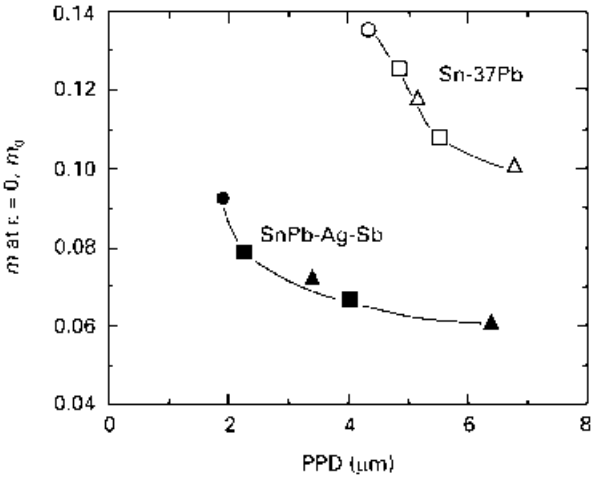

Figure 7 Relation between m_0 and average PPD of the two solder alloys, Sn–37Pb (○, □, △) and SnPb–Ag–Sb (●, ■, ▲). The PPD is changed by ageing at 353 K (□, ■) and 393 K (△, ▲). The data (○, ●) for the as-cast alloys are also shown.

3.1. Solders with ranked thermal fatigue properties

Fig. 8 shows the microstructure back-scattered electron image (composition) of each alloy in the as-cast state, aged at room temperature for 10 days after casting. In Sn–Pb eutectic system alloys, the coarsest structure is observed for Sn–37Pb. The alloyed solder showed a finer structure than Sn–37Pb however, Sn–36Pb–2Ag gives a finer lamellar structure than alloyed solder does. The addition of silver is effective in obtaining a fine structure by dispersion of Ag_3Sn. Sn–10Pb consisted of primary tin (dark phase) and eutectic, showing a large amount of lead phase (light phase) in the eutectic structure. Pb–50In forms only a lead-rich solid solution under the equilibrium state [26]; however, it shows an indium-rich phase (α) (dark phase) in addition to the lead-rich solid solution (light phase). The α-phase seems to be produced by peritectic reaction [26]. Sn–3.5Ag shows a fine dispersion of Ag_3Sn (light phase).

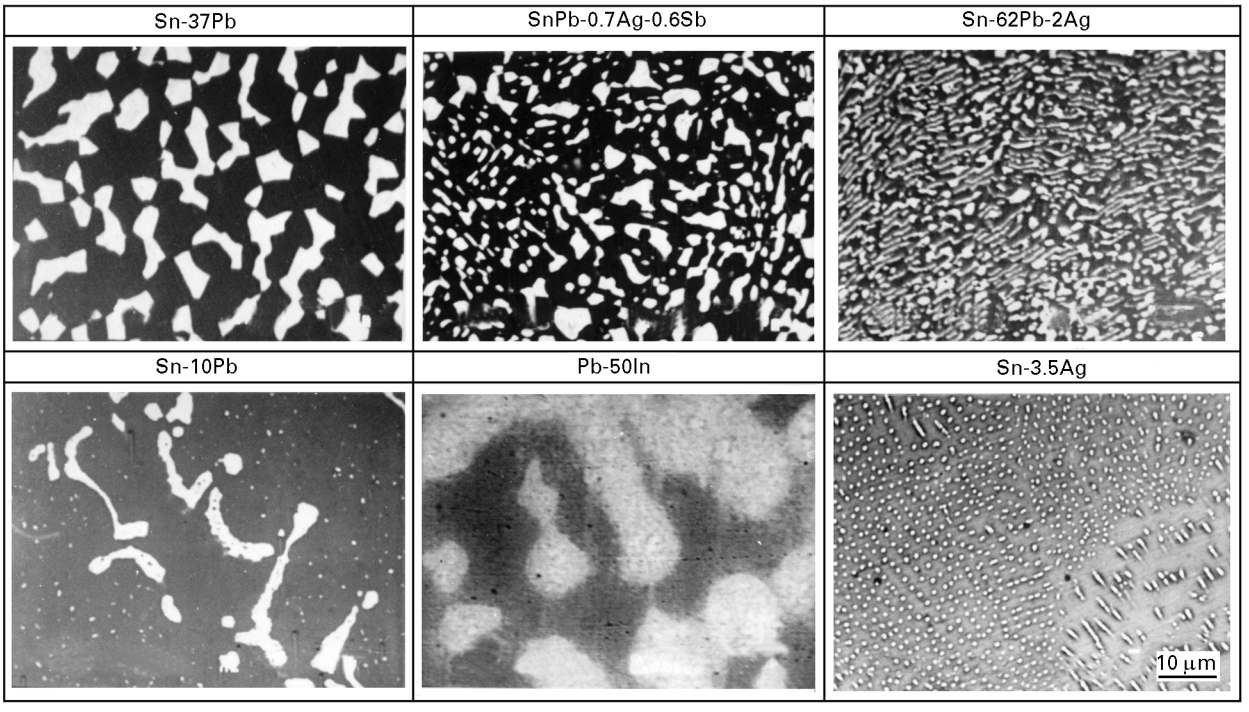

Figure 8 Back-scattered electron images (composition) of solders with ranked TFPs.

TABLE II Tensile strengths and elongations of solder alloys with different ageing conditions

Solder alloy	Tensile strength (MPa) for the following ageing conditions			Elongation (%) for the following ageing conditions		
	As cast; room temperature for 10 days	393 K for 605 ks	393 K for 1800 ks	As cast; room temperature for 10 days	393 K for 605 ks	393 K for 1800 ks
Sn–37Pb	44.4	42.2	42.5	41.0	46.4	51.1
SnPb–Ag–Sb	69.1	42.3	41.6	17.2	36.4	39.5
Sn–36Pb–2Ag	57.1	49.2	51.5	31.9	28.8	34.0
Sn–10Pb	37.1	27.2	30.5	15.1	27.1	24.0
Pb–50In	33.7	30.9	27.4	27.2	18.2	18.3
Sn–3.5Ag	28.1	17.8	19.0	27.4	36.9	36.3

Table II shows the tensile strength and elongation of several solders with different rankings of TFPs. On the whole, Sn–Pb eutectic-based solders have higher strengths than do the Sn–10Pb, Pb–50In and Sn–3.5Ag solders. The two solders ranked as poor in Table I showed higher strengths, irrespective of the ageing conditions. Sn–3.5Ag with excellent properties has the lowest strength in all ageing conditions. Ageing at 393 K decreased the tensile strength of all solders.

The elongations shown in Table II indicate that ageing at 393 K increased the elongation with the exception of SnPb–Ag–Sb and Pb–50In. On the whole, the elongation of each solder was increased after ageing at 393 K with the exception of Pb–50In, where ageing at 393 K decreased the elongation. For SnPb–2Ag and Sn–10Pb, elongation was drastically increased after ageing for 605 ks.

Fig. 9 shows plots of m_0 for several solders with different TFPs; the ranking is based on that in [5]. The m_0 for Sn–37Pb eutectic solder with the lowest resistance showed the largest value in all heat treatment conditions. m_0 gradually decreased with increasing resistance to thermal fatigue except for Sn–3.5Ag with the highest resistance. The tendency is almost the same irrespective of the heat treatment. In all ageing conditions, m_0 decreased with increasing ageing time except for Sn–3.5Ag, where m_0 was maintained almost constant; the decrease in m_0 might correspond to coarsening of the microstructure.

Fig. 10 shows the k value for all solders. The k value of the as-cast condition gradually decreased with increasing thermal fatigue resistance with exceptions of the SnPb–Ag–Sb and Sn–10Pb alloys. The Sn–10Pb alloy showed a large k in the as-cast condition, but the values after heat treatment became small. The relation between k and thermal fatigue ranking is almost good after ageing at 393 K for 1800 ks; the alloys with higher resistance have lower k. Thermal fatigue testing enhances the microstructure evolution by applying temperature and strain; therefore, the values after ageing are more significant than those in the as-cast condition.

On the whole, it can be concluded that the values of m and k are good measures for estimating the thermal fatigue resistance of solder alloys; the lower values indicate excellent TFPs; it is especially useful to consider both factors simultaneously. For example, the m_0 of Sn–3.5Ag is rather large in spite of the excellent resistance. However, the k value is extremely low. Accordingly, the equation to estimate the thermal fatigue resistance should be established by the use of m_0 and k with certain coefficients, respectively. The coefficients depend on the thermal fatigue test conditions such as the strain and temperature ranges, the maximum temperature, the frequency of the thermal cycle, the holding time, etc.

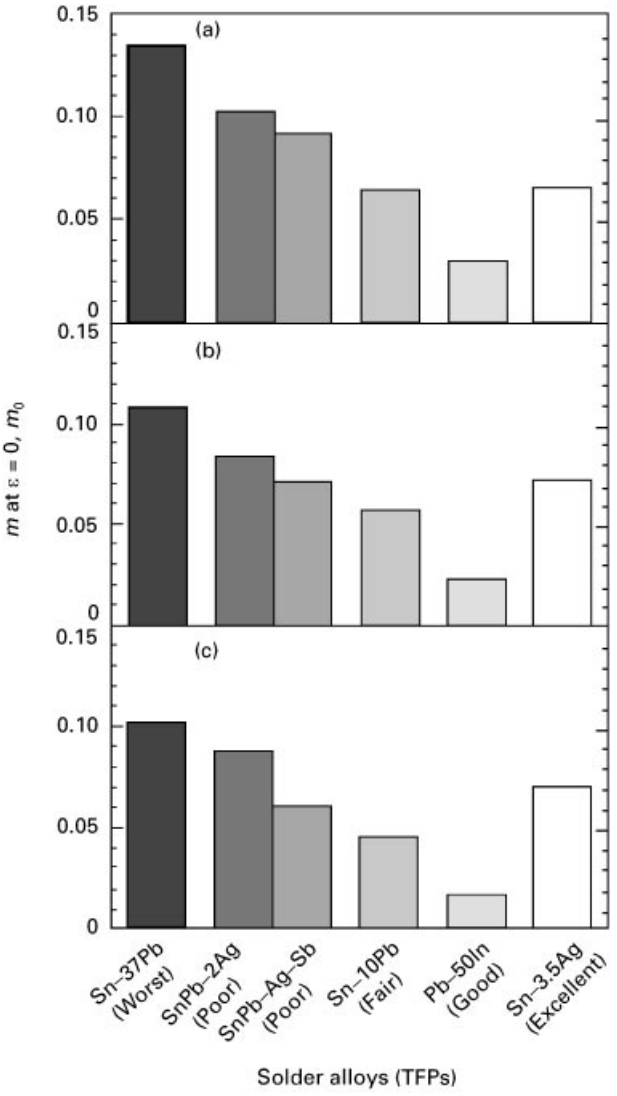

Figure 9 Plots of m at zero strain, m_0, of solder alloys with ranked TFPs: (a) as cast; (b) aged at 383 K for 605 ks; (c) aged at 393 K for 1800 ks.

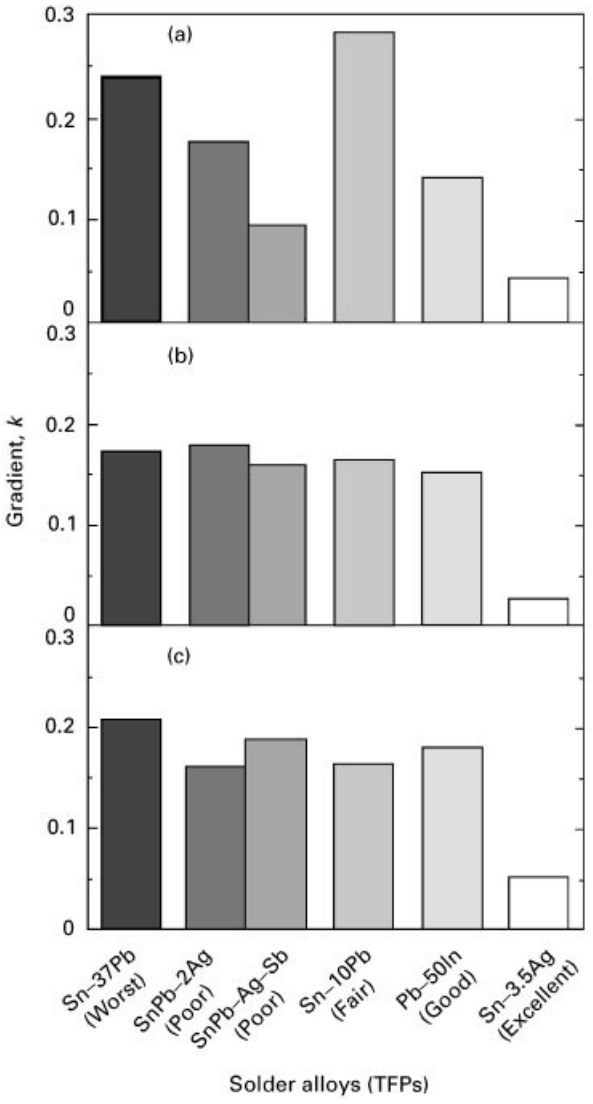

Figure 10 Gradient, k, of solder alloys with ranked TFPs; (a) as cast; (b) aged at 383 K for 605 ks; (c) aged at 393 K for 1800 ks.

More precise discussion will be required to explain the relation between the TFPs and values m_0 and k; however, the TFPs could be estimated by measuring these values. The proposed method is believed to be effective for developing the new thermal-fatigue-resistant lead-free solders.

4. Conclusions

A tensile test to obtain the SRSI, m, is proposed in order to estimate the TFPs of solder alloys. The method based on the comparison of m values would be effective for estimating the TFPs of solder alloys, although more detailed experiments will be necessary to establish a more accurate correlation. The results obtained are summarized as follows.

1. The alloyed solder with a small amount of silver and antimony in Sn–37Pb alloy has a higher tensile strength, lower elongation and superior thermal fatigue resistance to eutectic solder.

2. The plots of m against strain where m is measured showed a straight-line relationship in all solders tested. The m value at zero strain, m_0, decreases with ageing at an elevated temperature; the decreasing rate is larger for higher-temperature ageing. Also the value became small after a long ageing time, which corresponds to coarsening of microstructure. m_0 is closely related to the PPD; m_0 gradually decreased with increasing PPD. The relation holds for both eutectic and alloyed solders.

3. Tensile tests on several alloys with ranked TFPs revealed that m_0 and k are good measures for estimating the TFPs of solder alloys. The m_0 and k values of thermal-fatigue-resistant solder alloys are lower than those with poor resistance. It is recommended that the values after ageing are used for comparison of TFPs between solders. The TFPs could be estimated by evaluating both m_0 and k simultaneously, and in particular the values after ageing.

Acknowledgement

The authors express their hearty thanks to Nihon Genma Mfg Co., Ltd for preparation of the test specimens.

References

1. R. STRAUSS, in "Surface mount technology" (Butterworth–Heinemann, Oxford, 1994) p. 10.
2. R. P. PRASAD, in "Surface mount technology, principles and practice" (Van Nostrand Reinhold, New York, 1989) p. 3.
3. C. CAPILLO, in "Surface mount technology; materials, processes, and equipment" (McGraw-Hill, New York, 1990) p. 3.
4. R. R. TUMMALA and E. J. RYMASZEWSKI, in "Microelectronics Packaging Handbook" (Van Nostrand Reinhold, ed. by R. R. Tummala and E. J. Rymaszewsri, New York, 1989) p. 42.
5. C. LEA, in "A scientific guide to surface mount technology" (Electrochemical Publishing Ltd., Ayr, Scotland, 1988) p. 424.
6. D. R. FREAR, in "Solder mechanics, a state of the art assessment", edited by D. R. Frear, W. B. Jones and K. R. Kinsman, (Metallurgical Society of AIME, Warrendale, PA, 1991) p. 191.
7. J. W. MORRIS, JNR, D. TRIBULA, T. S. E. SUMMERS and D. GRIVAS, in "Solder joint reliability – theory and applications", edited by J. H. Lau (Van Nostrand Reinhold, New York, 1991) p. 225.
8. B. T. LAMPE, *Welding J.* **55** (1976) 330-s.
9. Y. YOSHIURA, H. CHAKI, T. TAKEMOTO and Y. KIKUCHI, in "Proceedings of the Second Symposium on Microjoining and Assembly Techniques in Electronics" (Japan Welding Society, 1996) p. 167.
10. Y. TANAKA, E. ASADA, Y. YOKOTA, A. NAKAMURA, H. ISHIDA and S. HARA, in "Proceedings of the Second Symposium on Microjoining and Assembly Techniques in Electronics" (Japan Welding Society, 1996) p. 173.
11. P. G. HARRIS and M. A. WHITEMORE, *Circuit World* 19 (1993) No. 2, 25, 32.
12. W. B. HAMPSHIRE, *Soldering & Surface Mount Technol.* No. 14 (1993) 49.
13. I. AITAKI, A. M. JACKSON and P. T. VIANCO, *ibid.* No. 20 (1995) 27.
14. K. AKINADE, R. BURGESS, M. CAMPBELL, S. CARVER, L. SANDERSON, R. WADE and C. MELTON, *ibid.* No. 20 (1995) 50.
15. W. B. MORRISON, *Trans. AIME*, **242** (1968) 2221.
16. B. P. KASHYAP and G. S. MURTY, *Mater. Sci. Engng* **50** (1981) 205.
17. S. W. ZEHR and W. A. BACKHOFEN, *Trans. Am. Soc. Metals* **61** (1968) 300.

18. R. W. ROHDE and J. C. SWEARENGEN, *J. Engng Mater. Technol.* **102** (1980) 207.
19. M. C. SHINE, L. R. FOX and J. W. SOFIA, *Brazing & Soldering* No. 9 (1985) 11.
20. H. D. SOLOMON, *ibid.* No. 11 (1986) 68.
21. H. E. CLINE and T. H. ALDEN, *Trans. AIME*, **239** (1967) 710.
22. D. H. AVERY and W. A. BACHHOFEN, *Trans. Am. Soc. Metals* **58** (1965) 51.
23. B. P. KASHYAP and G. S. MURTY, *Metall. Trans. A* **13** (1982) 53.
24. C. J. THWAITES, *Brazing Soldering* No. 11 (1986) 22.
25. W. J. TOMILSON and P. A. ROGERS, *J. Mater. Sci.* **22** (1987) 2416.
26. T. B. MASSALSKI, in "Binary alloy phase diagrams", Vol. 3, edited by H. Okamoto, P. B. Subramanian and L. Kacprzak (American Society for Metals, Metals Park, OH, 1990) p. 2269.

Received 13 May 1996
and accepted 20 January 1997